Published by
NIGERIAN SOCIETY OF PHYSICAL SCIENCES
Available online @ https://journal.nsps.org.ng/index.php/jnsps

J. Nig. Soc. Phys. Sci. 8 (2026) 3224

Journal of the Nigerian Society of Physical Sciences

A novel mathematical model for transmission dynamics of HPV and cervical cancer progression with cancer-reliant awareness

Ogechi Regina Amanso[a,b,*], Jeconia Okelo Abonyo[c], Phineas Roy Kiogora[c], Obiora Cornelius Collins[d]

[a] *Pan African University Institute for Basic Sciences, Technology and Innovation (PAUSTI), Nairobi, Kenya*
[b] *Kingsley Ozumba Mbadiwe University, Ideato South, Imo State*
[c] *Department of Mathematics, Jomo Kenyatta University of Agriculture and Technology, Nairobi, Kenya*
[d] *Institute of Systems Science, Durban University of Technology, Durban 4000, South Africa*

Abstract

Human papillomavirus (HPV) is a global health problem that causes the vast majority of cervical cancers. A novel mathematical model for HPV, as it progresses to cervical cancer, was formulated using a system of six ordinary differential equations that incorporates behavioural dynamics in the description of some control measures. In particular, this study introduces a novel chained dependency framework where the awareness parameter depends on Cancer burden, and the screening rate is a function of awareness. The essential epidemiological features of the model, such as the positivity and boundedness of the model, the basic reproduction number $\mathcal{R}_0$, the disease-free equilibrium, and the endemic equilibrium, are derived. The disease-free equilibrium is shown to be locally and globally asymptotically stable when $\mathcal{R}_0 < 1$. The endemic level of infection is expressed in terms of $\mathcal{R}_0$, and deductions are made from their relationship. Sensitivity analysis is conducted to determine which parameters are of utmost importance using a global sensitivity analysis method called the Partial Rank Correlation Coefficient (PRCC) method. Parameters are set from the literature, and simulation is carried out using the Runge–Kutta 4th order (RK4) method to explore the impact of various parameters on model dynamics. The results of the analyses not only reveal the impact of awareness campaigns, routine screening programmes, and vaccination in reducing HPV and cervical cancer, but also demonstrate how improved disease outcomes are directly linked to the chained awareness screening structure rather than the usual epidemic dynamics.

DOI:10.46481/jnsps.2026.3224

Keywords: Human papillomavirus, Cervical cancer, Mathematical modelling, Epidemiology, Awareness, Numerical simulation

Article History :
Received: 22 November 2025
Received in revised form: 20 December 2025
Accepted for publication: 18 February 2026
Available online: 22 March 2026

Communicated by: B. J. Falaye

1. Introduction

Human papillomavirus (HPV) is a serious global health concern responsible for a large percentage of cervical cancer cases, the fourth most common type of cancer among women in the world [1]. About 99.7% of cervical cancer cases are caused by long-term infection with HPV [2], and sadly, about 80% of sexually active women will get at least one type of HPV at some point in their lifetime without them knowing they have it [3]. HPV is a sexually transmitted disease that spreads from an infected person to a susceptible individual, mostly through vaginal, oral, or anal transmission [4], and certain strains called the "high-risk" types usually cause cancer in both men and women [5]. According to the African Union, the prevalence of

*Corresponding author: Tel. No.: +234-81-4444-2449;
Email address: regina.amanso@komu.edu.ng (Ogechi Regina Amanso)

HPV is substantially higher in Africa, and African countries bear the most significant burden of cervical cancer worldwide [6]. Cervical Cancer is the cancer that starts from the lower, narrow end of the uterus, and it was estimated by the Africa Health Organisation (AHO) that 72,000 cases of cervical cancer is caused by HPV every year in Africa. They also estimated that 34 out of 100,000 women are diagnosed with cervical cancer and 23 out of 100,000 women die from cervical cancer every year [7, 8]. As a matter of fact, in 2022 alone, 23% of global cervical cancer mortality was linked to Africa implying that approximately 153 000 lives were claimed by the illness [9]. Several factors have been attributed to this high cervical cancer burden in Low and Middle Income Countries (LMICs) of which poor knowledge, lack of screening and treatment programmes are not exempted. Even though there are vaccines that have been manufactured to prevent some HPV infections, including the high-risk ones [10], one major factor which is cited as one that keeps affecting HPV vaccine uptake remains inadequate knowledge regarding HPV, its vaccine, and the fact that it could lead to cervical cancer in women after a prolonged infection [11]. Thus, this work incorporates these important control measures that clearly stand for public enlightenment or awareness about HPV and its vaccine, treatment for only pre-cancerous lesions (since there is no cure for HPV itself [12]), and screening in its model formulation to study their impacts on HPV transmission and control.

Mathematical modelling serves as an important tool for analysing the dynamics and control of diseases and informing public health policy for improved disease management. Compartment-based models have been successfully used to study HPV transmission and its progression to cervical cancer. For instance, Lakoande *et al.* [13] formulated a two-sex mathematical model that shed more light on the transmission of HPV and how it progresses to Cervical Cancer. Their study birthed the idea that addressing vertical and same-sex transmission pathways will go a long way to curb HPV spread, which can subsequently reduce cervical cancer cases and mortalities. Some existing models have incorporated vaccination, screening, or both to measure the effectiveness of interventions. Zhang *et al.* [14], for instance, formulated a compartmental model that is made up of a system of ten Ordinary Differential Equations (ODEs) incorporating vaccination and screening parameters. The result of their research shows that increasing the vaccination rate is the best way to reduce the basic reproduction number. Earlier models are not left behind in this area, as researchers like Lee and Tameru [15] came up with a model to explain cervical cancer progression from HPV infection. The impact of vaccination in eliminating HPV could be seen in their work, and their result showed that intensifying the preventive approach and treatment can curb HPV spread. Ren *et al.* [16] in a more recent study showed a development of an advanced age-structured model that matches the World Health Organization elimination approach .

These innovative models however made use of fixed parameters to represent their control and preventive strategies, failing to capture the dynamic behavioural responses of subpopulation groups to the disease prevalence when in reality, public health measures to control infections or diseases are often influenced by the illness burden; for example, an intensified awareness campaign can be triggered by an increase in cases of cervical cancer, which will subsequently promote the likelihood of other women to want to undergo screening for HPV/Cervical dysplasia/Cervical Cancer.

To the best of our knowledge, the models that have been cited in this work, including recent ones for describing HPV spread and cervical cancer progression [17–21], have yet to consider awareness and screening in a chained dependency structure. For this reason, this research paper presents a system of six ordinary differential equations that extends the classical Susceptible-Infected-Recovered (SIR) framework to model the progression of cervical cancer from persistent High-risk HPV infection. This model provides an important novel contribution, which is the inclusion of behavioural dynamics in the description of two important control parameters, namely, the awareness and screening parameters. The awareness parameter depends on the number of cases of cervical cancer, and the screening rate is mathematically modelled as a function of the awareness probability.

This model also has a compartment that includes women with all stages of Cervical Intra-epithelial Neoplasia, that is, CIN-1, CIN-2, and CIN-3. This provides the room to account for early-stage medical interventions that are capable of stopping Cancer progression. This agrees with existing methods of stopping cervical cancer progression [1]. The model formulated in this study successfully deals with gaps in existing models by incorporating these dynamic behavioural responses in its control parameter description. This undoubtedly provides a new and reasonable perspective on HPV control and cervical cancer prevention that is useful in Africa and global settings.

This novel contribution, as stated earlier, is absent in existing mathematical models on HPV and Cervical Cancer progression because they made use of fixed intervention parameters. We believe that the chained behavioural framework makes modelling intervention dynamics more realistic. We utilize the fourth-order Runge-Kutta (RK4) approach for numerical simulations to study the behaviour of the model.

This paper is organized as follows: Section 1.1 contains the conceptual framework of the model, which explains the novel chain dependence structure. Section 1.2 entails the model formulation, the schematic diagram of the model, including the system of Ordinary Differential Equations ODE and behavioural dynamics. Section 2 details the model analysis. Parameter values and results are provided in Section 3. Section 4 discusses simulation results, and Section 5 concludes with implications of our results for public health policy and recommendations for future research.

1.1. The model's conceptual framework

The awareness parameter is a probability value in this study, denoted by k, which represents the probability of being informed about HPV and vaccine existence and availability. This probability is based on the number of cases of cervical cancer $C(t)$ using a logistic function to ensure that $k \in (0, 1)$. The screening rate, denoted by τ, which accelerates movement from the precancerous lesion class (P) to the removed class (R) is mathematically modelled as a function of awareness probability k, which demonstrates the impact of awareness on screening behaviour.

In summary, a chained dependency is presented. That is, a situation where k depends on the state variable C and τ relies on k as represented below:

$$C(t) \to k \to \tau. \tag{1}$$

To briefly explain the chained dependency structure, we have defined C as the compartment that houses women with Cervical Cancer. This chain dependence is logical in the sense that it is consistent with a realistic public health response loop where a rise in cervical cancer cases would naturally cause an increase in HPV and its vaccine campaign awareness programmes. Also, a rise in awareness campaigns would naturally lead to an increase in the rate at which women would want to go for screening.

1.2. Model development

A mathematical model in the form of non-linear ordinary differential equations is formulated, comprising: the Susceptible women S, the Infectious women I, women with precancerous conditions (CIN) P, Cervical Cancer cases C, Treated cases T, and the Removed class R. Table 1 summarizes the model compartments. The model is based on the following assumptions:

1. The total population is not constant
2. Women of 15 years old and above get recruited into the S compartment at the rate of Λ.
3. The C compartment comprises all-stage cervical cancer individuals, and they are capable of dying as a result of the disease at the rate of δ.
4. The screening rate depends on awareness probability, which in turn depends on state variable $C(t)$.
5. An aggregate high-risk HPV model is formulated without distinguishing genotypes.
6. The T compartment still undergoes screening to treat relapses early, and so they are assumed not to participate in HPV transmission.
7. All parameters are positive.
8. The Recovered and Vaccinated Individuals are permanently immune to an HPV-strain.

In the susceptible compartment, women get recruited into it at the rate of Λ. The susceptible individuals contract HPV through intimate skin-to-skin sexual interaction, denoted by β, and move to the I compartment, facilitated by the absence of awareness campaign probability $(1-k)$. Susceptible females get vaccinated at the rate of γ_3 depending on the awareness probability k and move to the R compartment. Infected individuals can either recover naturally at a rate γ_1 or proceed to the P compartment at rate α_2. Folks at P either undergo screening at the rate of τ and move to T at rate θ or advance to C in the absence of screening. The flow diagram of the model is displayed in Figure 1.

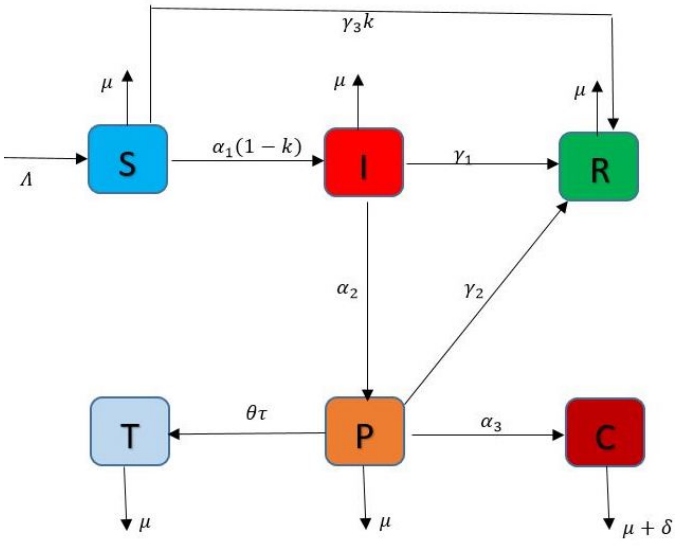

Figure 1. Schematic diagram of HPV–cervical cancer model.

The corresponding system of equations is as follows:

$$\begin{aligned}
\frac{dS}{dt} &= \Lambda - \alpha_1(1-k)S - \gamma_3 kS - \mu S,\\
\frac{dI}{dt} &= \alpha_1(1-k)S - \mu I - \gamma_1 I - \alpha_2 I,\\
\frac{dP}{dt} &= \alpha_2 I - \theta\tau P - \mu P - \alpha_3 P - \gamma_2 P,\\
\frac{dC}{dt} &= \alpha_3 P - (\mu+\delta)C,\\
\frac{dT}{dt} &= \theta\tau P - \mu T,\\
\frac{dR}{dt} &= \gamma_2 P - \mu R + \gamma_3 kS + \gamma_1 I,
\end{aligned} \tag{2}$$

where the force of infection α_1 is frequency dependent because the contact rate does not depend on population size

$$\alpha_1 = \frac{\beta\alpha_4(I+P+C)}{N}, \text{ with } \alpha_4, \tag{3}$$

representing the rate at which female folks acquire new sexual partners each year and β as the parameter that stands for the male-to-female transmission rate of HPV. From these definitions, it is pertinent to note that the male population is not vividly modelled in this work to ensure simplicity, but there is an implicit inclusion of male-to-female transmission through the incorporation of effective transmission parameters (denoting realistic transmission route), which happens to be consistent with the HPV modelling approach utilized in [14]. The total population, N is defined in (9). The description of model variables and parameters is presented in Table 1 and Table 2, respectively.

The screening rate τ $(0 < \tau < 1)$ depends on the probability of awareness k. Mathematically, $\tau(k) = min(1, \tau_0 + nk)$.

Where τ_0 = baseline screening rate per year, which stands for the minimum rate of screening without any awareness campaign, and n represents the dimensionless screening sensitivity, a parameter that determines how strongly the awareness k increases the screening rate τ.

Also, the probability of awareness k depends on the Cervical Cancer cases $C(t)$. This is given by:

$$k(C(t)) = \frac{1}{1 + e^{-(k_0 + mC(t))}}. \tag{4}$$

So it stays between 0 and 1, where k_0 is the dimensionless baseline awareness parameter and m is the awareness sensitivity. Since the enlightenment or awareness probability value, k, has been stated to depend on the cervical cancer occurrence in the population, the biological implication of this parameter can not be overemphasized, as it clearly:

- reduces infection through the factor $\alpha_4(1 - k)$,
- increases vaccination uptake of the susceptible female folks by a factor $\gamma_3 k$,
- and promotes screening campaigns through the relationship: $\tau(k) = min(1, \tau_0 + nk)$.

Table 1. Descriptions of the state variables.

State Variable	Description
S	Susceptible women population
I	Population of women infected with high-risk HPV types
P	Population of women with precancerous lesions (CIN 1–3)
T	Population of treated cases of precancerous lesions of the cervix
C	Population of women with all-stage cervical cancer
R	Population of removed/recovered individuals.

The population of removed/recovered individuals includes women who recover naturally from HPV and who have been vaccinated against the virus.

Table 2. Description of the model parameters.

Parameter	Description
Λ	Recruitment rate into susceptible women compartment
μ	Natural death rate of human
β	Transmission rate of HPV from male to female
α_4	Rate at which females acquire new sexual partners per year
τ $(0 < \tau < 1)$	Screening rate
γ_1	Recovery rate of infected women
α_3	Exit rate from P (CIN) compartment to C compartment
k	Probability of being enlightened about HPV/vaccine
$1 - k$	Probability of not being enlightened
α_1	Rate at which susceptible women get infected with high-risk HPV types.
γ_3	Vaccination rate of Susceptible individuals
θ	Movement rate of women with precancerous lesions into the treatment compartment T
α_2	Rate at which infected women develop cervical precancerous lesions.
δ	Mortality rate as a result of cervical cancer
$\tau(k)$	Awareness dependent screening rate
τ_0	Minimum screening rate without awareness campaign.
n	Screening sensitivity that determines how strongly the awareness k affects the screening rate τ.
$k(C)$	Probability of awareness.
k_0	Baseline awareness parameter.
m	Awareness sensitivity.

The awareness and screening parameters have been assumed to lie between 0 and 1 to model realistic expectations; When k is 1, it implies that all susceptible individuals are aware of the HPV and its vaccines. This means that there will be no infection, which is realistically not possible. When it is equal to 0, it means that no susceptible person is aware of the disease and the vaccine's existence, which is also unrealistic. A similar reasoning can be applied to the screening parameter τ. When it is 0, no one goes for screening, meaning that all individuals in P progress to Cervical Cancer. When it is 1, it means that every individual in P gets screened immediately at the fastest rate possible. This is unrealistic in the real public health settings due to issues like limited health care capacity, screening delays, and refusals, etc.

2. Analysis of the model

2.1. Basic properties of the model

2.1.1. Positivity

In this section, we prove that all the model variables are non-negative. This will ensure that the system of (2) is mathematically well-posed and valid in a defined domain Ω defined by

$$\Omega = \{(S, I, P, C, T, R) \in \mathbb{R}^6 \mid S > 0, I \geq 0, P \geq 0, C \geq 0, T \geq 0, R \geq 0\}. \tag{5}$$

The positivity of the state variables of model (2) is summarized in the Theorem below.

Theorem 2.1. [Positivity of Solutions] Let the admissible region be defined as

$$\Omega = \{(S, I, P, C, T, R) \in \mathbb{R}^6_+\}, \tag{6}$$

where $\mathbb{R}^6_+$ stands for the non-negative orthant. If the boundary conditions $(S(0), I(0), P(0), C(0)), T(0), R(0)$ lie in domain Ω, then the solutions $S(t)$, $I(t)$, $P(t)$, $C(t)$, $T(t)$ and $R(t)$ remain non-negative for all time $t > 0$.

Hence, the region Ω is positively invariant under the model dynamics.

Theorem 2.1 is established using the standard analytical method as shown in [14, 22].

To start with, initial values are assumed positive: $S(0) > 0$, $I(0) \geq 0$, $P(0) \geq 0$, $C(0) \geq 0$, $T(0) \geq 0$, $R(0) \geq 0$. It is also assumed that the model (2) equations are continuous, implying that the state variables change smoothly with time.

Since the solutions are continuous, it means that a dependent variable could only become negative if it first becomes zero and then its derivative, or rate of change at that moment, is negative, so it would move below zero.

To examine any possibility of this happening, the values of each derivative in model (2) when its corresponding state variable is equated to 0 are observed:

$$\begin{aligned}
S = 0 &\Rightarrow \frac{dS}{dt} = \Lambda > 0, \\
I = 0 &\Rightarrow \frac{dI}{dt} = \alpha_1(1 - k)S \geq 0, \\
P = 0 &\Rightarrow \frac{dP}{dt} = \alpha_2 I \geq 0, \\
C = 0 &\Rightarrow \frac{dC}{dt} = \alpha_3 P \geq 0, \\
T = 0 &\Rightarrow \frac{dT}{dt} = \theta\tau P \geq 0, \\
R = 0 &\Rightarrow \frac{dR}{dt} = \gamma_2 P + \gamma_3 kS + \gamma_1 I \geq 0.
\end{aligned} \tag{7}$$

It is observed above that all the derivatives at the vanishing point are either zero or positive, which means that none of the variables can move below zero. Any state variable that gets to zero will either stay at 0 or increase.

In conclusion, all the state variables (S, I, P, C, T, R) are never negative but remain positive at all time t provided the initial values are positive.

Mathematically, it means that the model solution will always remain inside the positive region:

$$\mathbb{R}^6_+ = \{(S, I, P, C, T, R) \in \mathbb{R}^6 : S, I, P, C, T, R \geq 0\}. \tag{8}$$

2.1.2. Boundedness

The boundedness of the total population N of model (2) is presented in this section. Particularly, we show that N stays within finite bounds as time increases to infinity. The total population N is given by:

$$N = S + I + P + C + T + R. \tag{9}$$

From the system of equations (2), we have:

$$\frac{dN}{dt} = \Lambda - \mu N - \delta C. \tag{10}$$

The upper bound is obtained in the absence of cancer cases, while the lower bound is obtained when the worst-case scenario is considered, that is, when $C = N$.

Mathematically, we have:

$$\Lambda - \mu N - \delta N \leq \frac{dN}{dt} \leq \Lambda - \mu N. \tag{11}$$

Solving for the bounds. Obtaining $N(t)$ by comparison theorem, gives

$$\frac{\Lambda}{\mu + \delta} \leq \liminf_{t\to\infty} N(t) \leq \limsup_{t\to\infty} N(t) \leq \frac{\Lambda}{\mu}. \tag{12}$$

This shows that the population stays within finite bounds as time t tends to infinity, in the presence and absence of Cancer cases in the model population.

2.2. Disease-free equilibrium

The disease-free Equilibrium (DFE) $X^0 = (S^0, I^0, P^0, C^0, T^0, R^0)$ is the critical point of the model (2) when there is no disease in the population [23]. At Equilibrium,

$$\frac{dS}{dt} = \frac{dI}{dt} = \frac{dP}{dt} = \frac{dC}{dt} = \frac{dT}{dt} = \frac{dR}{dt} = 0. \tag{13}$$

With this, the DFE X^0 of model (2) becomes

$$\begin{aligned} X^0 &= (S^0, I^0, P^0, C^0, T^0, R^0) \\ &= \left(\frac{\Lambda}{\gamma_3 k_* + \mu},\ 0,\ 0,\ 0,\ 0,\ \frac{\gamma_3 k S^0}{\mu}\right). \end{aligned} \tag{14}$$

where $k_* = k(0) = \frac{1}{1+e^{-k_0}}$.

Since the DFE is the point when there is no disease in the system, studying it helps us to understand the initial situation/starting point and whether the disease will invade the population when it comes into the system [24].

2.3. Basic reproduction number

The basic reproduction number denoted by $\mathcal{R}_0$ is the threshold parameter that is used to analyse the stability of the disease-free equilibrium [25]. It can be defined as the average number of secondary infections that will occur when one infected person is introduced into a completely susceptible environment [24]. The basic reproduction number, $\mathcal{R}_0$, is computed using the next generation matrix method as described in [26]. The infected classes I, P, and C are used to obtain the basic reproduction number. The rate at which new infections occur in the population is represented by $\mathcal{G}_i$, and the net changes that occur in the infected classes (excluding new infection entries) are represented by $\mathcal{L}_i$. They are mathematically provided below:

$$\mathcal{G} = \begin{bmatrix} \alpha_1(1-k)S(t) \\ 0 \\ 0 \end{bmatrix}, \quad -\mathcal{L} = \begin{bmatrix} -(\mu + \gamma_1 + \alpha_2)I(t) \\ \alpha_2 I(t) - (\theta\tau + \mu + \alpha_3 + \gamma_2)P(t) \\ \alpha_3 P(t) - (\mu + \delta)C(t) \end{bmatrix}. \tag{15}$$

The Jacobian of $\mathcal{G}$ and $\mathcal{L}$ evaluated at DFE is obtained as:

$$G = \begin{bmatrix} \frac{\beta\alpha_4\Lambda}{N(\gamma_3 k_* + \mu)} & \frac{\beta\alpha_4\Lambda}{N(\gamma_3 k_* + \mu)} & \frac{\beta\alpha_4\Lambda}{N(\gamma_3 k_* + \mu)} \\ 0 & 0 & 0 \\ 0 & 0 & 0 \end{bmatrix} \tag{16}$$

and

$$L = \begin{bmatrix} (\mu + \gamma_1 + \alpha_2) & 0 & 0 \\ -\alpha_2 & (\theta\tau + \mu + \alpha_3 + \gamma_2) & 0 \\ 0 & -\alpha_3 & (\mu + \delta) \end{bmatrix}. \tag{17}$$

The basic reproduction number $\mathcal{R}_0$ is the spectra radius of GL^{-1} which is obtained as:

$$\begin{aligned} \mathcal{R}_0 = &\frac{\beta\alpha_4}{N} \cdot \frac{\Lambda(1-k_*)}{(\gamma_3 k_* + \mu)(\mu + \gamma_1 + \alpha_2)} \\ &\times \left[1 + \frac{\alpha_2}{\theta\tau_* + \mu + \alpha_3 + \gamma_2} + \frac{\alpha_2\alpha_3}{(\theta\tau_* + \mu + \alpha_3 + \gamma_2)(\mu + \delta)}\right]. \end{aligned} \tag{18}$$

Note that τ has been expressed as τ_* in equation (18) above, since the basic reproduction number is expressed in DFE and τ is in terms of k, it is mathematically proper to express τ in terms of the DFE value of k. That is, $\tau(k_*) = min(1, \tau_0 + nk_*) = \tau_*$. Also, it is important to note that τ has been taken to be $0 < \tau < 1$ in $\mathcal{R}_0$ derivation.

Recall that $\frac{dN}{dt} = \Lambda - \mu N - \delta C$. At DFE, the total population $N_0 = \frac{\Lambda}{\mu}$. Taking this into consideration, the basic reproduction number can be rewritten as:

$$\begin{aligned} \mathcal{R}_0 = &\frac{\beta\alpha_4\mu(1-k_*)}{(\gamma_3 k_* + \mu)(\mu + \gamma_1 + \alpha_2)} \\ &\times \left[1 + \frac{\alpha_2}{\theta\tau_* + \mu + \alpha_3 + \gamma_2} + \frac{\alpha_2\alpha_3}{(\theta\tau_* + \mu + \alpha_3 + \gamma_2)(\mu + \delta)}\right]. \end{aligned} \tag{19}$$

When $\mathcal{R}_0 < 1$, HPV infection fizzles out with time. However when $\mathcal{R}_0 > 1$, the infection spreads over time [27].

2.4. Local stability of disease-free equilibrium

The rationale behind this section is to study the behaviour of the system with respect to the disease-free Equilibrium. This analysis reveals whether the infections will die out or persist when the disease is absent. From the system of equations 2, let the rate of appearance of new infections be denoted by $\mathcal{F}$.

$$\mathcal{F} = \begin{bmatrix} 0 \\ \alpha_1(1-k)S(t) \\ 0 \\ 0 \\ 0 \\ 0 \end{bmatrix}. \tag{20}$$

When $\mathcal{F}$ is set to 0, the force of infection term $\alpha_1(1-k)S$ contained in the second equation of the system of (2) disappears. The Jacobian of the resulting system of equations evaluated at DFE will then become:

$$J|_{DFE} = \begin{pmatrix} -(\gamma_3 k_* + \mu) & -\frac{\beta\alpha_4(1-k_*)S^0}{N_0} & -\frac{\beta\alpha_4(1-k_*)S^0}{N_0} & -\frac{\beta\alpha_4(1-k_*)S^0}{N_0} & 0 & 0 \\ 0 & -(\mu+\gamma_1+\alpha_2) & 0 & 0 & 0 & 0 \\ 0 & \alpha_2 & -(\theta\tau_* + \mu + \alpha_3 + \gamma_2) & 0 & 0 & 0 \\ 0 & 0 & \alpha_3 & -(\mu+\delta) & 0 & 0 \\ 0 & 0 & \theta\tau_* & 0 & -\mu & 0 \\ \gamma_3 k & \gamma_1 & \gamma_2 & -\frac{\gamma_3 S^0 m e^{k_0}}{(1+e^{k_0})^2} & 0 & -\mu \end{pmatrix}. \tag{21}$$

It can be observed that the eigenvalues of the matrix $J|_{DFE}$ are all negative real parts since all the parameters of the model are assumed to be positive. They are $-\mu$ (twice), $-(\gamma_3 k_* + \mu)$, $-(\mu+\delta)$, $-(\theta\tau_* + \mu + \alpha_3 + \gamma_2)$ and $(\mu + \gamma_1 + \alpha_2)$.

Therefore, from condition A5 in Van Den Driessche and Watmough (2002), The DFE of the Model in (2) is locally asymptotically stable [24].

2.5. Global stability of DFE

In this section, the conditions that ensure the system of equations (2), at DFE, is globally asymptotically stable when $\mathcal{R}_0 < 1$, using the Castillo-Chavez technique demonstrated in [13] is presented. These conditions ensure that, at DFE, when $\mathcal{R}_0 < 1$, the population compartments of the model in (2) return to DFE at any starting point.
Following the Castillo-Chavez method, the system is set:

- $X = (S, R)$ comprising the uninfected compartments
- $Z = (I, P, C, T)$ representing the infected compartments

The system can be written as:
$\dot{X} = F(X, Z)$, $\dot{Z} = G(X, Z)$
$F(X, Z)$ and $G(X, Z)$ are the uninfected and infected subsystems respectively. Next, the two required conditions associated with the Castillo-Chavez method are checked:

- $H1$: If $Z = 0$, that is, when there are no infections in system (2), then the subsystem X becomes:
  $\dot{S} = \Lambda - (\gamma_3 k + \mu)S$ and $\dot{R} = -\mu R + \gamma_3 k S$. At equilibrium, the system returns to DFE X^0 in (14).
- $H2$: Here, the condition that ensures the infection does not persist when $\mathcal{R}_0 < 1$ is shown. Here it is required that $\hat{G}(X, Z) \geq 0$. Where $\hat{G}(X, Z)$ refers to the non-linear, saturating section of the infected sub-system obtained using $AZ - G(X, Z)$. A is the Jacobian of the infected subsystem of the model (2).

To show $H2$:
The infected subsystem is:

$$G(X,Z) = \begin{bmatrix} \alpha_1(1-k)S(t) - (\mu+\gamma_1+\alpha_2)I(t) \\ \alpha_2 I(t) - (\theta\tau + \mu + \alpha_3 + \gamma_2)P(t) \\ \alpha_3 P(t) - (\mu+\delta)C(t) \\ \theta\tau P(t) - \mu T(t) \end{bmatrix}. \tag{22}$$

The linearized infection matrix at DFE, denoted as A, is:

$$A = \left.\frac{\partial G}{\partial Z}\right|_{X^0} = \begin{bmatrix} \frac{\beta\alpha_4(1-k)S^0}{N_0} - (\mu+\gamma_1+\alpha_2) & \frac{\beta\alpha_4(1-k)S^0}{N_0} & \frac{\beta\alpha_4(1-k)S^0}{N_0} & 0 \\ \alpha_2 & -(\theta\tau+\mu+\alpha_3+\gamma_2) & 0 & 0 \\ 0 & \alpha_3 & -(\mu+\delta) & 0 \\ 0 & \theta\tau & 0 & -\mu \end{bmatrix}. \tag{23}$$

The off-diagonal entries of the matrix A are non-negative. A is a Metzler-type Matrix and the Castillo - Chavez method expects this sign pattern.

$$AZ = \begin{bmatrix} \left[\frac{\beta\alpha_4(1-k)S^0}{N_0} - (\mu+\gamma_1+\alpha_2)\right]I(t) + \frac{\beta\alpha_4(1-k)S^0}{N_0}P(t) + \frac{\beta\alpha_4(1-k)S^0}{N_0}C(t) \\ \alpha_2 I(t) - (\theta\tau+\mu+\alpha_3+\gamma_2)P(t) \\ \alpha_3 P(t) - (\mu+\delta)C(t) \\ \theta\tau P(t) - \mu T(t) \end{bmatrix}. \tag{24}$$

Using Matrices AZ and the infected compartments $G(X, Z)$ above, $\hat{G}$ is obtained:

$$AZ - G(X,Z) = \hat{G}(X,Z) = \begin{bmatrix} \beta\alpha_4(1-k)(I(t)+P(t)+C(t))\left[\frac{S^0}{N_0} - \frac{S(t)}{N(t)}\right] \\ 0 \\ 0 \\ 0 \end{bmatrix}. \tag{25}$$

From above, $\hat{G}(X, Z) \geq 0$ if and only if $\frac{S^0}{N_0} \geq \frac{S(t)}{N(t)}$. If this inequality holds, then the H2 condition is satisfied, and the DFE is globally asymptotically stable when $\mathcal{R}_0 < 1$.

2.6. Endemic equilibrium point

The endemic equilibrium point (EEP) is the steady state at which disease is present in the population [28]. It is obtained by setting $\frac{dS}{dt} = \frac{dI}{dt} = \frac{dP}{dt} = \frac{dC}{dt} = \frac{dT}{dt} = \frac{dR}{dt} = 0$ and solving for the state variables, which are expressed in terms of parameters only or implicitly in terms

of one of the state variables [29]. From the results of the analysis, the endemic equilibrium points of the system of equations (2) expressed in terms of the parameters and the state variable I^* are

$$(S^*, I^*, P^*, C^*, T^*, R^*) = \left(\frac{\Lambda}{\alpha_1(1-k) + \gamma_3 k + \mu},\ I^*, \right. \\ \left. \frac{\alpha_2 I^*}{\theta\tau + \mu + \alpha_3 + \gamma_3}, C^*,\ T^*,\ R^* \right), \quad (26)$$

where

$$I^* = \frac{\Lambda - \frac{N(\gamma_3 k+\mu)(\mu+\gamma_1+\alpha_2)}{\beta\alpha_4\Phi(1-k)}}{\mu + \gamma_1 + \alpha_2},$$

$$C^* = \frac{\alpha_2\alpha_3 I*}{(\theta\tau + \mu + \alpha_3 + \gamma_3)(\mu + \delta)},$$

$$T^* = \frac{\theta\tau\alpha_2 I^*}{\mu(\theta\tau + \mu + \alpha_3 + \gamma_3)}$$

and

$$R^* = \frac{\gamma_3 P^* + \gamma_3 k S^* + \gamma_1 I^*}{\mu}.$$

For the EEP $(S^*, I^*, P^*, C^*, T^*, R^*)$ (equation (26)) to be biologically feasible, all the compartments have to be non-negative. Since all parameters are assumed to be positive, it can be observed that the EEP feasibility clearly depends on the sign of the infectious component I^* because from equation (26), $I^* > 0$ if and only if the numerator of its expression is positive, which occurs when $\mathcal{R}_0$ is more than a threshold value. Consequently, the EEP exists and is biologically meaningful whenever $R_0 > V$, where V denotes the endemicity threshold defined in the next section, (section 2.7). When $\mathcal{R}_0 \leq V$, the endemic equilibrium collapses to the disease-free equilibrium obtained in equation (14), implying that HPV and cervical cancer progression will not be sustained in the population.

2.7. Relationship between the infectious I compartment and the basic reproduction number

To further clarify the conditions under which the endemic equilibrium is biologically feasible, the explicit relationship between the endemic infection level I^* and the basic reproduction number R_0 will now be examined.

In this section, the relationship between the endemic level of infection I^* and the basic reproduction number ($\mathcal{R}_0$) is derived. This is very important in determining the impact of $\mathcal{R}_0$ on the spread of the infection. Let the basic reproduction number be rewritten as:

$$\mathcal{R}_0 = \frac{\beta\alpha_4\Phi_*\Lambda(1-k_*)}{N(\gamma_3 k_* + \mu)(\mu + \gamma_1 + \alpha_2)}, \quad (27)$$

where

$$\Phi_* = \left[1 + \frac{\alpha_2}{\theta\tau_* + \mu + \alpha_3 + \gamma_2} + \frac{\alpha_2\alpha_3}{(\theta\tau_* + \mu + \alpha_3 + \gamma_2)(\mu + \delta)} \right].$$

Then:

$$\mathcal{R}_0 = \frac{\Phi_*}{N} W, \quad (28)$$

which implies that

$$N = \frac{\Phi_* W}{\mathcal{R}_0}, \quad (29)$$

where

$$W = \frac{\beta\alpha_4\Lambda(1-k_*)}{(\gamma_3 k_* + \mu)(\mu + \gamma_1 + \alpha_2)}. \quad (30)$$

Using the above equations, I^* is expressed in terms of $\mathcal{R}_0$ as follows:

$$I^* = \Phi_* W \left[\frac{\Lambda}{\Phi_* W} - \frac{1}{\mathcal{R}_0} \right] \left[\frac{1}{\mu + \gamma_1 + \alpha_2} \right]. \quad (31)$$

This equation can also be written as:

$$I* = \frac{\Lambda\left[1 - \frac{V}{\mathcal{R}_0}\right]}{\mu + \gamma_1 + \alpha_2}, \quad (32)$$

where V is the endemicity threshold for $\mathcal{R}_0$ and is equal to: $\frac{\Phi_* W}{\Lambda}$. Since all the parameters are assumed to be positive, it implies that V is also positive. Thus, we can conclude the following:

- , if and only if $\mathcal{R}_0 > V$.
- The derivative

$$\frac{\partial I^*}{\partial \mathcal{R}_0} = \frac{\Phi_* W}{\mathcal{R}_0^2(\mu + \gamma_1 + \alpha_2)} \quad (33)$$

  is greater than 0, which implies that the endemic level I* increases monotonically with $\mathcal{R}_0$.
- As $\mathcal{R}_0$ tends to infinity, I* tends to

$$\frac{\Lambda}{\mu + \gamma_1 + \alpha_2} \quad (34)$$

  and as $\mathcal{R}_0$ tends to V^+, then I^* tends to zero.

2.8. Global sensitivity analysis

Sensitivity analysis of a mathematical model studies how variations in input parameters influence the model's output. The process can involve local or global approaches [30]. In this study, the global approach will be utilized. Global Sensitivity Analysis (GSA) is useful in studying how the changes in parameters across various valid ranges affect the behaviour of models, and it is also important in identifying the most influential parameters that contribute to disease transmission decrease or increase [31]. The Partial Rank Correlation Coefficients (PRCC) approach is applied here because of its efficiency in measuring the strengths and direction of the relationship between inputs and outputs, even when their relationship is non-linear [32]. Here, we will make use of the basic reproduction (19):

$$\mathcal{R}_0 = \frac{\beta\alpha_4\mu(1-k_*)}{(\gamma_3 k_* + \mu)(\mu + \gamma_1 + \alpha_2)} \\ \times \left[1 + \frac{\alpha_2}{\theta\tau_* + \mu + \alpha_3 + \gamma_2} + \frac{\alpha_2\alpha_3}{(\theta\tau_* + \mu + \alpha_3 + \gamma_2)(\mu + \delta)} \right]. \quad (35)$$

In this study, a plausible range of ±50% of the baseline values provided in Table 3 is applied in order to better reflect biological variability and uncertainty in the parameter. It is pertinent to note that PRCC values that are positive tend to increase the basic reproduction number when increased, and those with negative values reduce the basic reproduction number when their values are increased [33]. The result of the global sensitivity analysis is presented in Figure 2 in the form of a PRCC tornado plot.

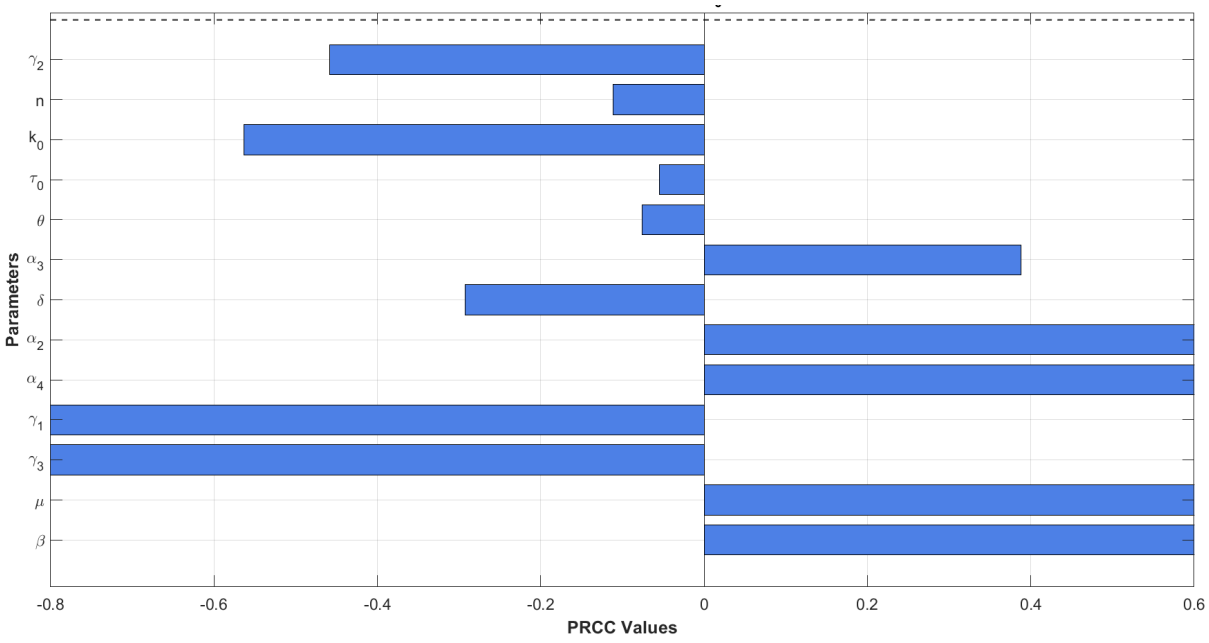

Figure 2. PRCC tornado plot.

From Figure 2, it can be seen that the baseline parameters τ_0 and k_0 are on the negative side of the tornado plot. This implies that an increase in these parameters gives rise to a decrease in $\mathcal{R}_0$. As a matter of fact, every parameter that lies on the negative side of the tornado plot causes a decrease in the basic reproductive number when increased, while the parameters on the positive side of the plot lead to an increase in $\mathcal{R}_0$ as they are increased. Meanwhile, it can be observed that the parameters k_* and τ_* do not appear in the PRCC plot. This is because they are not independent model inputs. Instead, they are expressions that clearly depend on the primitive parameters k_0, n, and τ_0:

$$k_* = \frac{1}{1+e^{-k_0}}, \qquad \tau_* = \min(1, \tau_0 + nk_*). \tag{36}$$

Since PRCC evaluates the effect of independent variation in input parameters on $\mathcal{R}_0$, only primitive parameters were included in the sensitivity analysis. The influence of k_* and τ_* is therefore captured indirectly through the sensitivities of their generating parameters (k_0, n, τ_0). From Figure 2, even though the natural recovery rate γ_1 and vaccination rate γ_3 appear to have the highest negative sensitivity, some of the other important parameters also have reasonably high negative sensitivities on $\mathcal{R}_0$. In descending order, they are: k_0, θ, and τ_0. This signifies the importance of not just vaccination, but baseline awareness rate, treatment rate, and baseline screening rate, in curbing disease spread. It means that, out of the intervention parameters introduced in the formulated model, vaccination plays the major role (consistent with [14] conclusion) in curbing the disease spread, followed by baseline awareness, treatment (matching result in [15]), and screening, respectively.

On the right side of the plot, however, α_4 and β (amongst others) appear to have very high sensitivities on $\mathcal{R}_0$, indicating that any increase in these parameters will yield an increase in $\mathcal{R}_0$. In the real-world context, it means that an increase in the rate at which individuals acquire new sexual partners and in the rate of transmission of HPV will give rise to the disease spreading more over time. This result is consistent with realistic expectations.

3. Results

We utilize a numerical simulation to gain deeper insight into the qualitative behaviour of our proposed model because of its non-linear nature. The classical fourth-order Runge-Kutta (RK4) method is used in this study to approximate the trajectories of the system. The RK4 approach offers a good balance between computational efficiency and accuracy. Numerical simulations are carried out over a limited time interval [0, T], with given initial conditions- $S \geq 0, I \geq 0, P \geq 0, C \geq 0, T \geq 0, R \geq 0$.

3.1. Values of parameters and state variables

The model will be simulated utilizing these initial conditions that are derived from realistic assumptions about population subgroups. The parameter values used for the simulations are summarized in Table 3. The results are obtained with the parameter values provided in Table 3. Meanwhile, the basic reproduction number $\mathcal{R}_0$, estimated using the parameter values in Table 3 is $0.1347 < 1$. For the initial values for the population classes, recall that at DFE, $\frac{dN}{dt} = 0$, $N = N_*$, and $C = 0$ in the equation $\frac{dN}{dt} = \Lambda - \mu N - \delta C$. This means that $N_* = \frac{\Lambda}{\mu}$ and using the parameter values $N_* = 556$. Now, assuming 100 initially infected individuals, that is, $I(0) = 100$. We take $P(0) = 100, T(0) = 56, S(0) = 200, C(0) = 0$ and $R(0) = 100$.

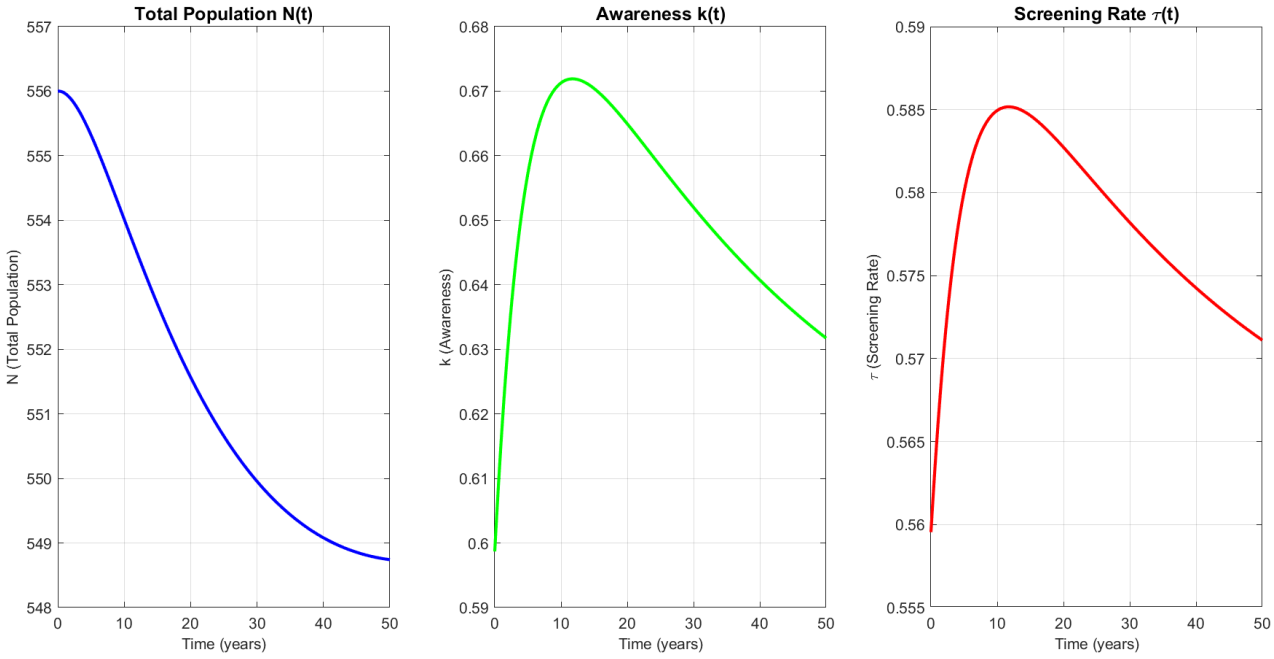

Figure 3. Population, awareness, and screening dynamics over time.

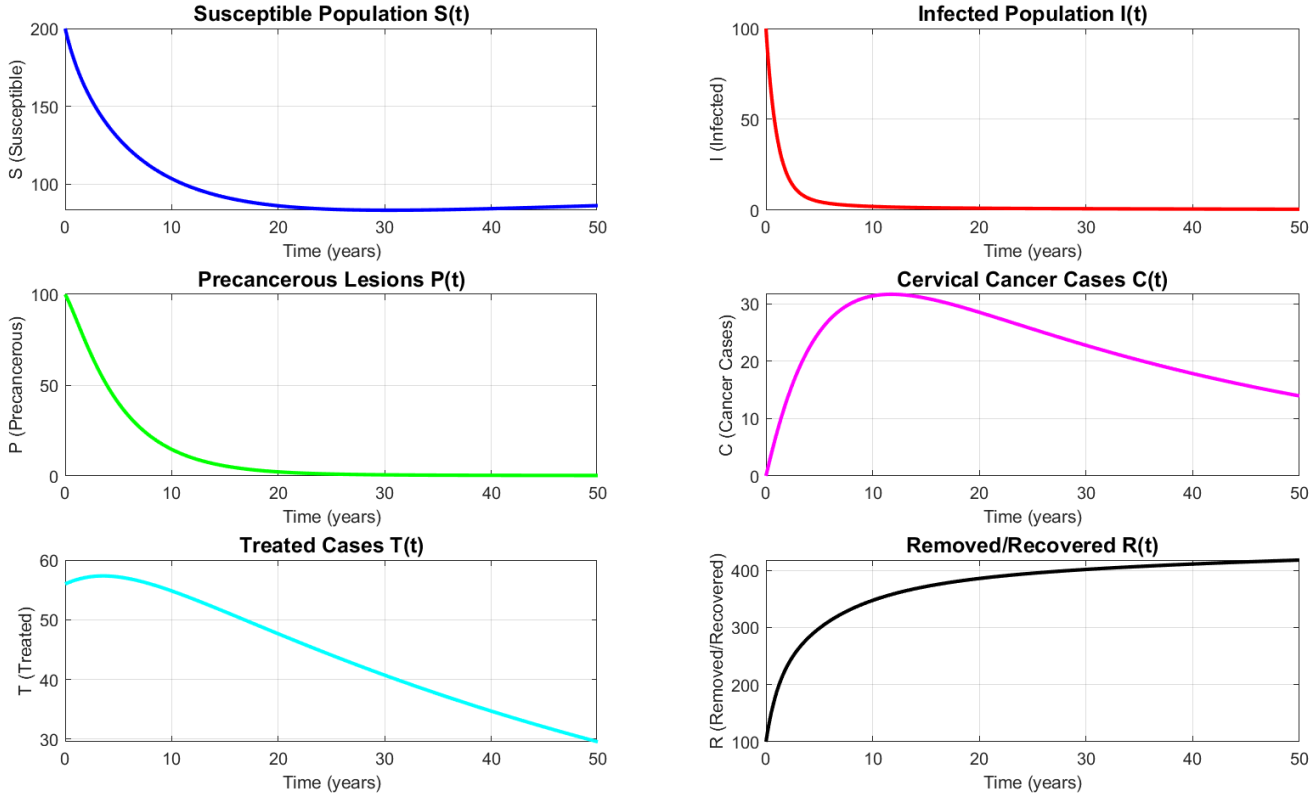

Figure 4. Dynamics of state variables over time.

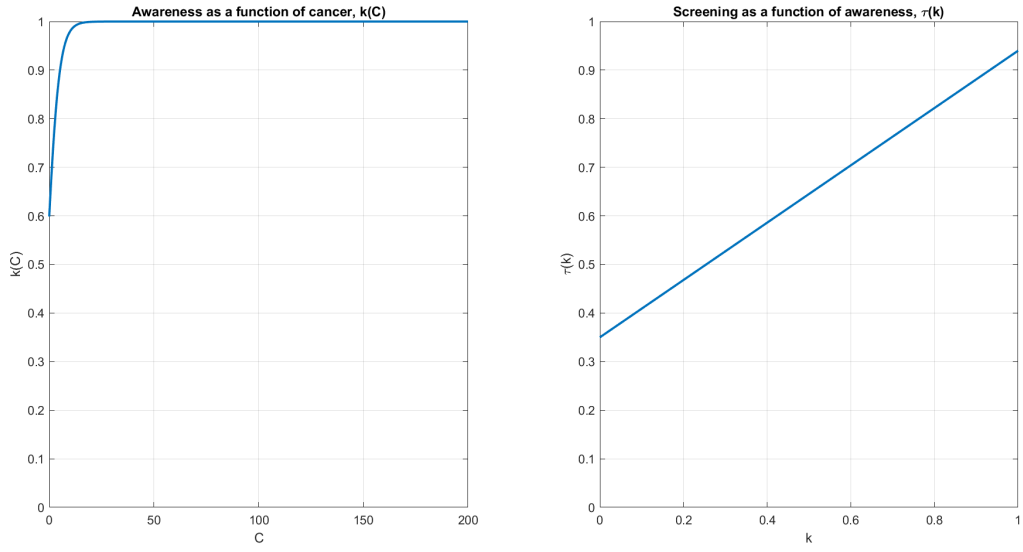

Figure 5. (a) Functional relationship plot of $\tau(k)$ and $k(C)$.

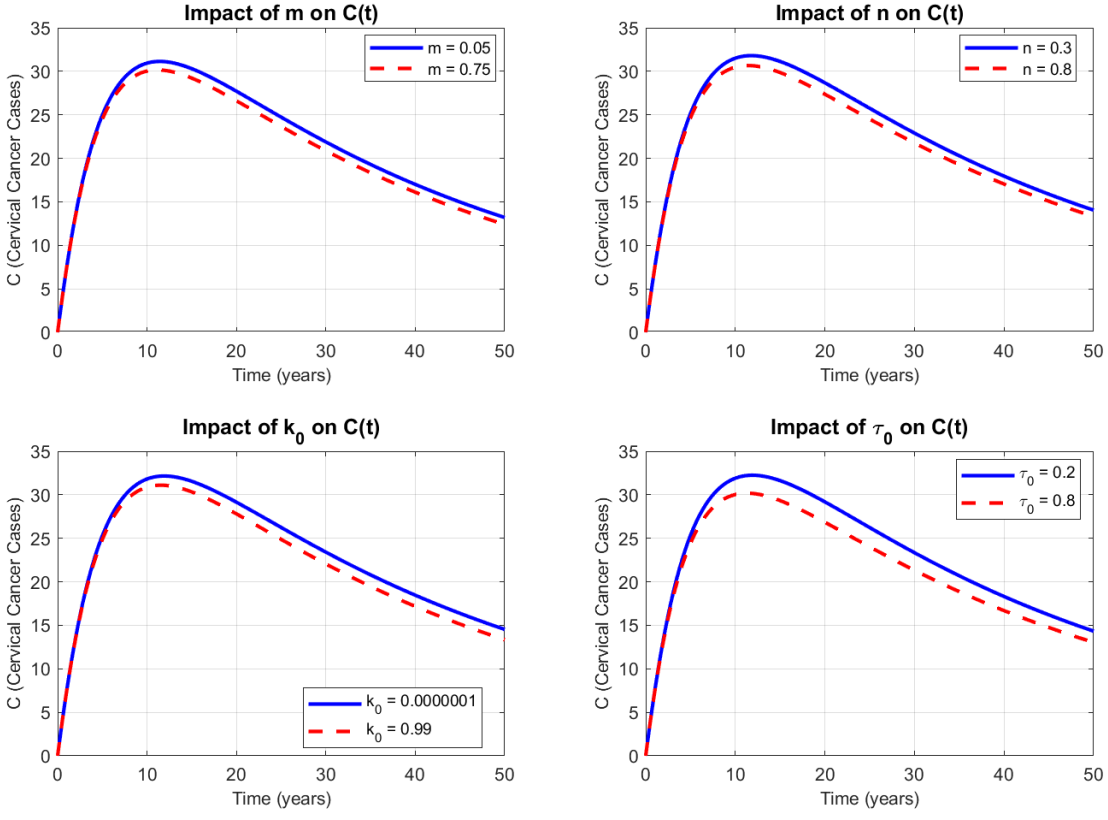

Figure 5. (b) Scenario comparisons for $C(t)$.

Figure 5. (a) Functional relationship plot of $\tau(k)$ and $k(C)$. (b) Scenario comparisons for $C(t)$.

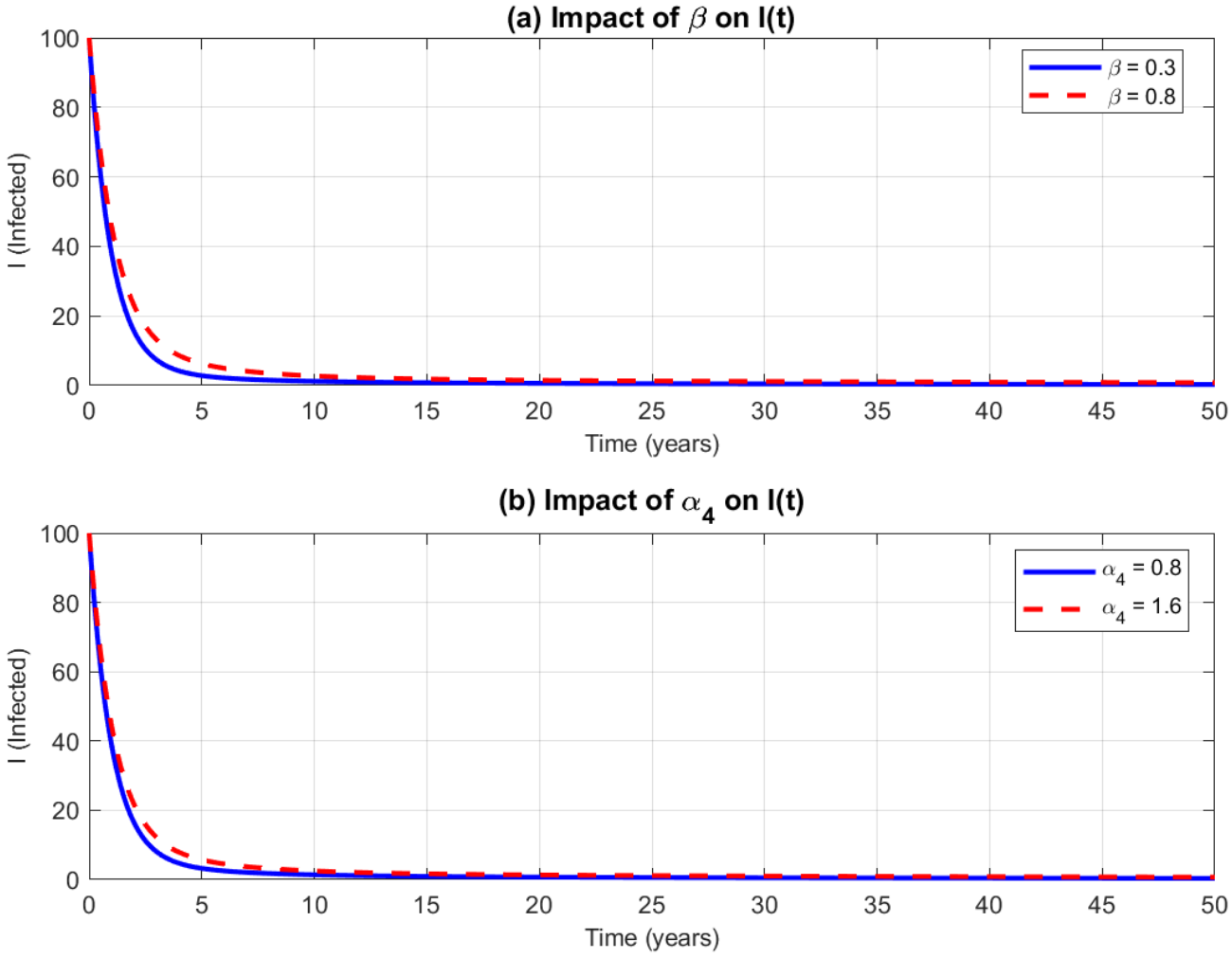

Figure 6. Effects of β and α_4 on Infectious compartment.

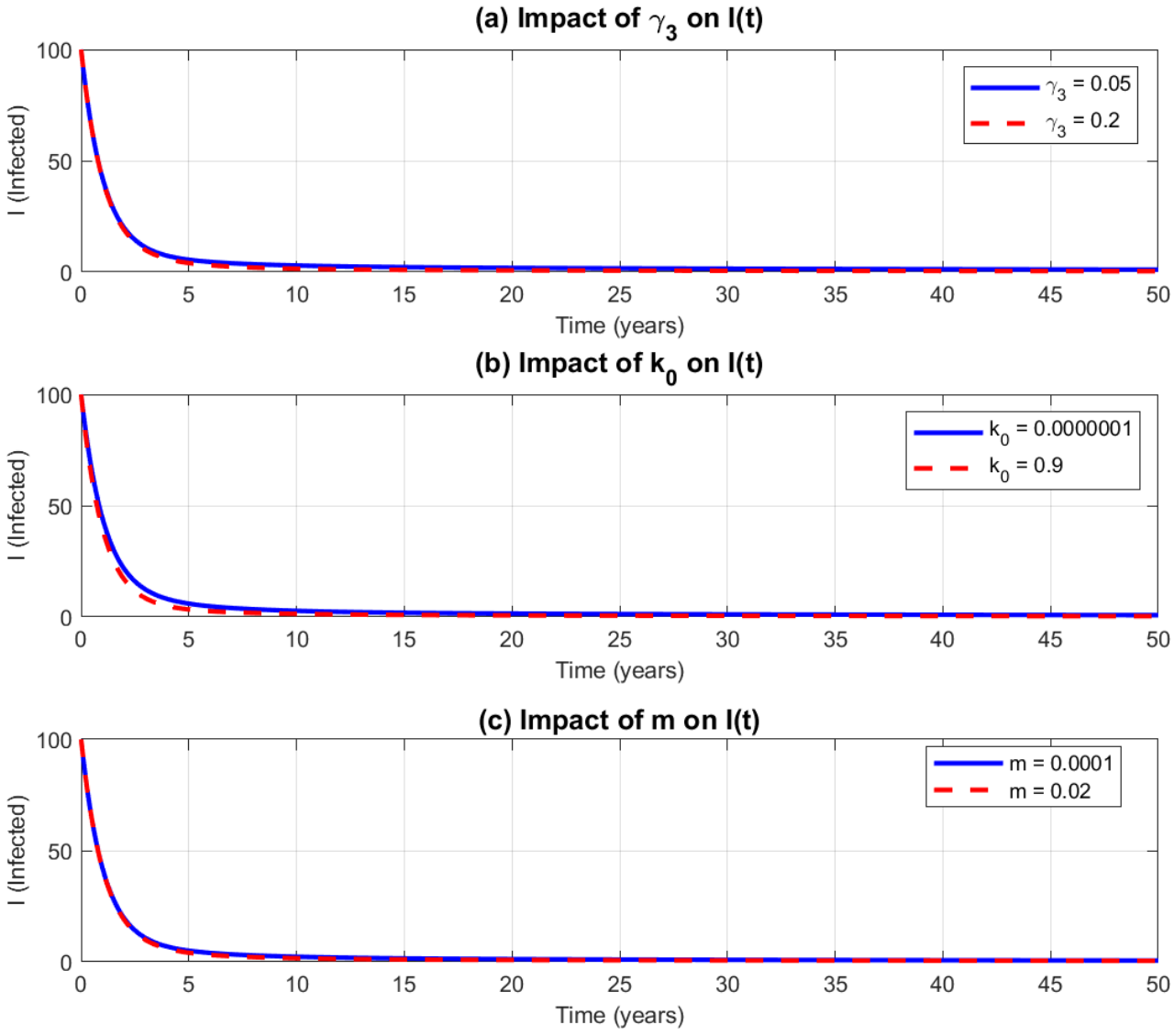

Figure 7. Effects of γ_3, k_0 and m on Infectious compartment.

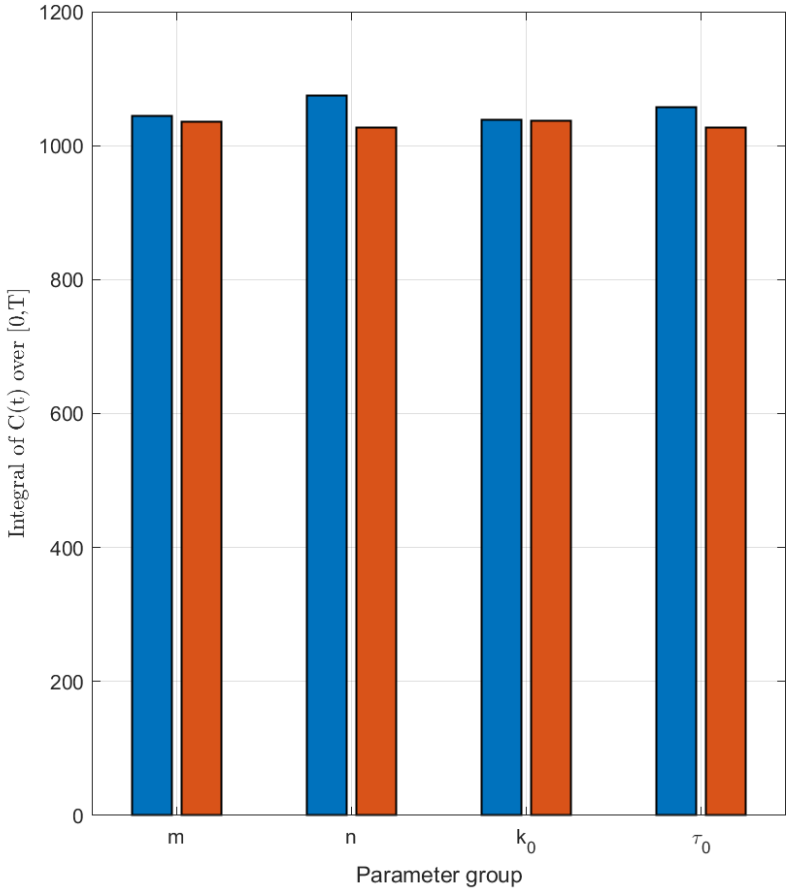

Figure 8. Total cancer burden (area under $C(t)$).

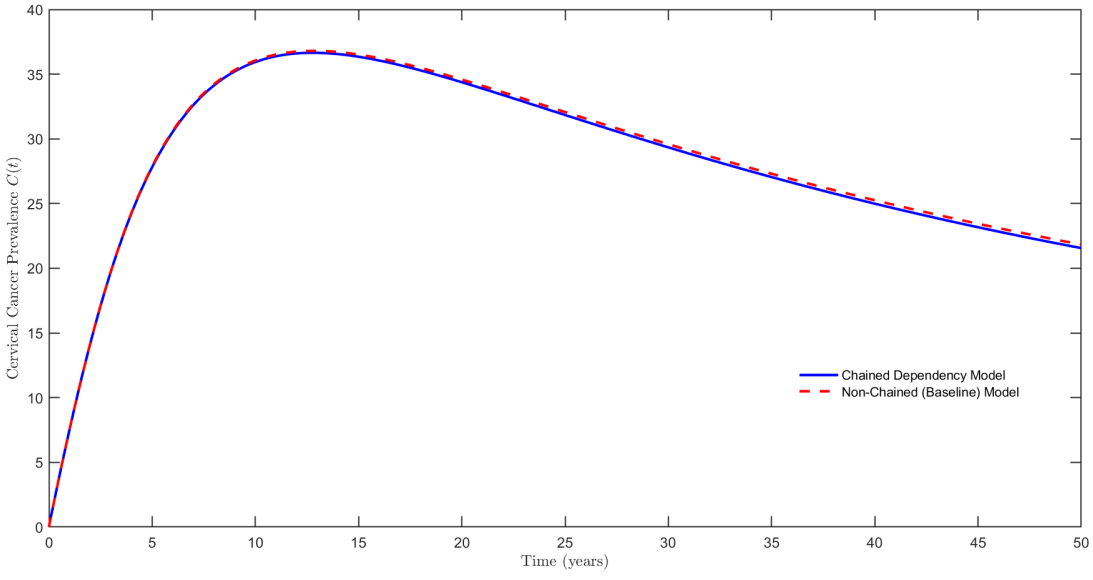

Figure 9. Cervical cancer dynamics under a chained awareness–screening model compared with a baseline model with fixed awareness and screening rates.

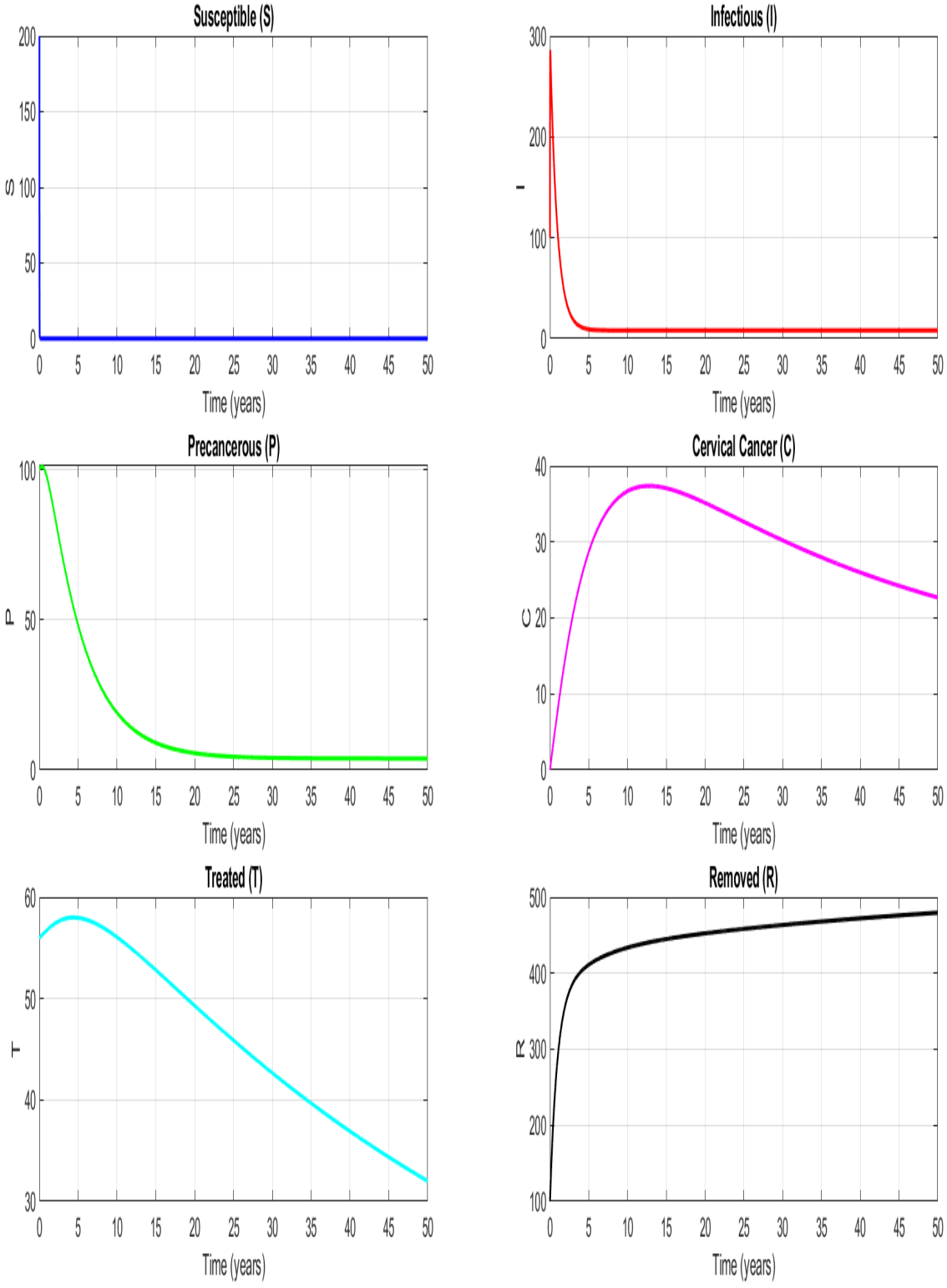

Figure 10. Dynamics of the state variables when $R_0 > 1$.

Table 3. Parameter values used in the model with corresponding sources.

Symbol	Selected Value	Source
β	0.556000	[34]
Λ	9.016228	[34]
μ	0.016200	[14]
γ_3	0.125000	Assumed
γ_1	0.990000	[14]
α_4	1.250000	Assumed
α_2	0.100000	[14]
δ	0.010000	[14]
α_3	0.080000	[14]
θ	0.030000	Assumed – 30% of CIN2/3 cases treated annually in a moderate screening context
k	0.600000	Assumed – 60% awareness in a moderately educated population with active national campaigns
τ_o	0.350000	Assumed baseline annual screening rate of 35% without awareness campaigns
τ	0.150000	Assumed 15% increase in screening as a result of awareness campaigns
k_o	0.400000	Assumed initial awareness value of 40% in the population
m	0.0100000 (Dimensionless)	Assumed
n	0.350000	Assumed
γ_2	0.100000	Assumed
k_*	0.590000	Estimated using $k_* = k(0) = \frac{1}{1+e^{-k_0}}$
τ_*	0.556500	Estimated from $\tau(k_*) = \min(1, \tau_0 + nk_*)$ (capped below 1 for realism)

4. Discussion

The first set of plots is presented in Figure 3. - The Far left of the figure shows how the total population changes with time. Indicates that the population gradually becomes stable and does not go to zero or blow up unrealistically as time goes on.
The middle plot in Figure 3 shows how awareness increases greatly as cancer cases rise, but stabilizes as time goes on, demonstrating limits that are realistically connected to the natural way a real population responds.
The third plot (far right) in Figure 3 provides information on how screening evolves with time. Screening gets to its peak at 10 years as awareness campaign increases, but gradually stabilizes as time goes on.

In Figure 4, the susceptible S reduces gradually and becomes reasonably low due to movement of individuals from that compartment to the R compartment (due to vaccination/awareness) for $\mathcal{R}_0 = 0.1347 < 1$. The infected I decreases for $\mathcal{R}_0 = 0.1347 < 1$ largely due to the majority of them recovering naturally and moving to the R compartment. Some of them still move to the P compartment. The C gets to its peak at 10 years but reduces gradually after 10 years due to reduced inflow from the P compartment and disease-induced, as well as natural death rates. The pre-cancer compartment reduces as individuals move to the treatment compartment and develop cervical cancer. The T class gets to a peak value at time 5 years when screening increases and then reduces afterwards through natural means μ. The removed/recovered compartment R increases due to vaccination and natural recovery.

In Figure 5 (a), the first graph (left) shows that awareness campaign increases as cancer cases increase. It can be observed that it has a fast increase initially, but stays at a constant level, almost touching 1. Also, the second graph (right of figure 5 (a)) shows that screening $\tau(k)$ increases as awareness increases, with screening growing steadily towards full uptake; The graph indicates that $\tau = 0.35$ when $k = 0$ and $\tau = 0.94 < 1$ when $k = 1$, respecting realistic expectations.

It is observed from Figure 5 (b) that high values of the sensitivity and baseline parameters lead to the reduction of cervical cancer cases at a faster pace, while lower values of these parameters give rise to more cases of cancer, but later reduces as time goes on for $\mathcal{R}_0 = 0.1347 < 1$ when parameter values in Table 3 values are utilized.

In Figure 6 (a), consistent with realistic expectation, the disease for high and low values of β eventually declines with time when $\mathcal{R}_0 = 0.1347 < 1$. This matches the result in [13] that highlighted the importance of addressing transmission pathways. It can even be observed in Figure 6 (a) that the β parameter with a lower value causes the disease to fizzle out faster than those with higher values, which is also consistent with realistic expectations.
Figure 6 (b) shows that the disease dies out gradually for $\mathcal{R}_0 = 0.1347 < 1$ at different values of α_4. However, matching realistic expectations, the disease ends faster at a lower value of α_4.

Figure 7 (a) it is shown that vaccination facilitates the movement of individuals from susceptible (S) to the recovered class R, consistent with the impact of vaccination on disease spread highlighted in [15]. In line with this, individuals move out faster from I compartment at a higher rate of γ_3 when $\mathcal{R}_0 = 0.1347 < 1$.
Also, a careful look at Figure 7 (b) shows that for $\mathcal{R}_0 = 0.1347 < 1$, the baseline awareness parameter, at a higher value, causes infection to die out faster, and at a lower value, makes infection decrease at a slower rate. This also matches realistic expectations.

In Figure 7 (c), higher awareness sensitivity m, causes infection to decrease faster. Recall that m is the parameter that determines how strongly the cancer burden increases awareness campaign. This also indirectly suggests that higher campaign awareness induced by cancer burden will lead to a decrease in the long run.

In Figure 8, the blue bar indicates low values of the parameters under consideration, giving rise to higher cancer burden, while the red bar stands for high parameter (highlighted on the vertical axis) values that lead to lower cervical cancer burden. This is in line with realistic expectations because it implies that when the individuals are more enlightened, and screening is stronger (both at baseline and when awareness increases), the total number of cancer incidences reduces. This further highlights the importance of the inclusion of awareness campaigns and screening programmes in the health sector concerned with reducing the total cervical cancer burden.

To display the impact of the novel chained dependency framework introduced in this study, the dynamics of the cervical cancer compartment under two different modelling assumptions will be studied, see Figure 9. In the first scenario, awareness is modelled as a function of cervical cancer burden, and the screening rate is subsequently defined as a function of awareness, forming a chained feedback mechanism. In the second setting, the awareness parameter and screening rate are taken to be constant over time, representing a baseline model without behavioural feedback. In order to ensure a fair comparison, the same parameter values and initial conditions are utilized in both cases.

Figure 9 shows what happens over time to cervical cancer cases under the two scenarios described above. The results show that both models display similar behaviour at early times, since cancer burden is initially low and awareness-driven effects are very little. However, as cervical cancer cases increase, the chained dependency model (represented by the blue curve in Figure 9) produces a slightly lower peak cancer burden and a faster decline when compared to the model without the chained dependency framework. This occurs because higher cancer cases increase awareness, and this, in turn, amplifies screening and consequently reduces disease progression. The baseline model, represented by the red chain curve, which lacks this feedback mechanism, displays a cancer prevalence that appears to be consistently higher. These results demonstrate that the improved disease outcomes are tied directly to the chained awareness-screening framework rather than standard epidemic dynamics.

Figure 10 shows the dynamics of the population classes with respect to time when the basic reproduction number $\mathcal{R}_0 = 2.44 > 1$. The transmission rate of HPV β and the rate of acquisition of new sexual partners were increased to 11.235 each, while other parameters were kept the same. The Susceptible population S can be seen to get exhausted quicker compared to the dynamics when $\mathcal{R}_0 < 1$ in Figure 4. The curve appears to drop sharply at the beginning and immediately flattens, and appears like a straight line very close to zero. The Infectious population I gets to a peak close to 300 and immediately reduces and gets to a constant value. With other classes, when $R_0 > 1$, the disease keeps spreading in the population and does not fizzle out with time. The Precancerous P compartment does comes decreases and comes to a steady positive level, a little above zero, as individuals migrate to the Treated compartment and some recover naturally. The Cancer C individuals increase and later experience a very slight decrease as time goes on as a result of small values of α_3, μ, and δ. Small α_3 provides a slow progression from P class to C class, and small values of μ and δ gave rise to the very slow out-flow of individuals out of C. The treatment T curve increases slightly and briefly, and then starts slowly decrease afterwards as individuals migrate due to natural death. The recovered population R increases as they receive inflow of individuals from I, P, and S compartments due to natural recovery and vaccination.

5. Conclusion

In this research article, we formulated a system of six ordinary differential equations to explain the transmission dynamics of Human Papillomavirus and its progression to Cervical Cancer. In the formulated model, a novel approach where the awareness campaign relies on the number of Cervical Cancer cases and where the Screening rate depends on the intensity of the awareness campaign was incorporated, leading to a chained dependency in the model formulation.
The analytical result shows that when the basic reproduction number $\mathcal{R}_0 < 1$, the disease-free equilibrium state is stable. The epidemiological implication is that the disease can be eradicated provided $\mathcal{R}_0$ remains less than unity. Also, the endemic equilibrium state exists if and only if R_0 is greater than some endemicity threshold V. So, control measures that will keep $\mathcal{R}_0 < 1$ are strongly recommended for the chances of disease eradication.
The parameters that are capable of decreasing the value of $\mathcal{R}_0$ are shown clearly in Figure 2 of subsection 2.8 when the global sensitivity analysis was conducted. Global sensitivity analysis and plots from varying baseline and sensitivity parameters $(, n, k_0, \tau_0)$ show that these parameters, alongside the vaccination parameter γ_3 are important control measures in curbing HPV transmission and subsequently, reducing cervical cancer cases.
Numerical simulation indicates that HPV and Cervical Cancer burden reduces over time when vaccination, awareness and screening increases. The simulation results reveal the crucial roles of conduct-driven measures in controlling the transmission dynamics of HPV and its progression to Cervical Cancer.

Based on the results of this research, Encouraging vaccination uptake in the community will play a great role in reducing the transmission of HPV, as also suggested in [14]. Even though the model was formulated utilizing some simplified assumptions, it still offers some specific recommendations supporting awareness campaigns and screening programmes, which are most likely to result in notable reductions in overall cervical cancer burden. Thus, policymakers should encourage organizing free or subsidized screening programs and intensifying awareness as a priority in reducing cervical cancer burden. Summarily, Implementing combined preventive and control measures- vaccinating individuals, intensifying awareness campaigns, and screening programmes in communities will go a long way to curb HPV transmission and cancer progression over time.

The model formulated in this study utilizes simplified population dynamics, literature-based parameters, and parameters estimated

from related literature.

Future research could focus on using real epidemiological data in the model, incorporating a particular strain of HPV, and applying optimal control theory in order to determine how to control the disease with minimum cost.

Acknowledgment

My sincere gratitude goes to the African Union Commission for granting me the scholarship opportunity to be able to carry out this research, which has provided me with the opportunity to give research-based suggestions that can curb HPV spread and reduce the occurrence of cervical cancer.

6. Data availability

In this study, no primary datasets were generated or collected. The data used were parameter values that was obtained from published literature and assumptions, clearly stated in Table 3

References

[1] World Health Organization, "Cervical cancer fact sheet", (2025). https://www.who.int/news-room/fact-sheets/detail/cervical-cancer.

[2] K. S. Okunade, "Human papillomavirus and cervical cancer", Journal of Obstetrics and Gynaecology 40 (2020) 602–608. https://doi.org/10.1080/01443615.2019.1634030.

[3] Office on Women's Health, "Human papillomavirus", (2024). https://womenshealth.gov/a-z-topics/human-papilloma-virus.

[4] National cancer institute, "HPV and Cancer", (2025). https://www.cancer.gov/about-cancer/causes-prevention/risk/infectious-agents/hpv-and-cancer.

[5] Cleveland Clinic, "HPV (Human Papilloma Virus)", (2023). https://my.clevelandclinic.org/health/diseases/11901-hpv-human-papilloma-virus.

[6] African Union, CARMMA, "Human papillomavirus (HPV) in africa", (2022). https://carmma.au.int/en/news/press-releases/2022-06-02/human-papillomavirus-hpv-africa.

[7] Africa Health Organisation, "Cervical cancer in africa fact sheet", (2024). https://aho.org/fact-sheets/cervical-cancer-in-africa-fact-sheet/.

[8] National cancer Institute, "What Is cervical cancer?", (2022). https://www.cancer.gov/types/cervical.

[9] The World Bank, "Preventing cervical cancer in africa: Why scaling HPV vaccination is a priority", (2024). https://blogs.worldbank.org/en/health/Preventing-cervical-cancer-in-Africa-Why-scaling-HPV-vaccination-priority.

[10] Cleveland clinic, "HPV vaccine", (2024). https://my.clevelandclinic.org/health/treatments/21613-hpv-vaccine.

[11] I. Nzisa, R. Kamenwa, J. Orwa & P. Samia, "Knowledge of human papillomavirus vaccine as a determinant of uptake among guardians of adolescent girls: A single hospital experience in nairobi, kenya", Global Pediatrics **12** (2025) 100249. https://doi.org/10.1016/j.gpeds.2025.100249.

[12] National Health Service (NHS), "Human papillomavirus (HPV)", (2022). https://www.nhs.uk/conditions/human-papilloma-virus-hpv/.

[13] J. Lakoande, O. W. Sawadogo & A. Kiemtore, "Mathematical modelling and numerical simulation of the dynamics of human papillomavirus (HPV) and cervical cancer in Burkina Faso", Asia Pacific Journal of Mathematics **12** (2025) 1. https://doi.org/10.28924/APJM/12-8.

[14] K. Zhang, X. Wang, H. Liu, Y. Ji, Q. Pan, Y. Wei & M. Ma, "Mathematical analysis of a human papillomavirus transmission model with vaccination and screening", Mathematical Biosciences and Engineering **17** (5) (2020) 5449–5476. https://doi.org/10.3934/mbe.2020294.

[15] S. Lee & A. M. Tameru, "A mathematical model of human papillomavirus (HPV) in the United States and its Impact on cervical cancer", Journal of Cancer **3** (2012) 262. https://doi.org/10.7150/jca.4161.

[16] H. Ren, R. Xu & J. Zhang, "HPV transmission and optimal control of cervical cancer in China", Scientific Reports **15** (2025) 21354. https://doi.org/10.1038/s41598-025-05514-y.

[17] N. Althobaiti & D. Baleanu, "Dynamics of human papillomavirus (HPV) incorporating homosexual transmission and HPV-induced cancers", Advances in Continuous and Discrete Models **104** (2025) 23. https://doi.org/10.1186/s13662-025-03957-1.

[18] H. D. Desta, G. T. Tilahun, T. M. Tolasa & M. G. Geleso, "Mathematical model of human papillomavirus (HPV) dynamics with double-dose vaccination and its impact on cervical cancer", Discrete Dynamics in Nature and Society **2024** (2024) 1. https://doi.org/10.1155/ddns/9971859.

[19] Y. He, "Advances in HPV-associated cervical cancer dynamic modelling for prevention and control evaluation", China CDC Weekly **7** (2025) 225. https://weekly.chinacdc.cn/en/article/doi/10.46234/ccdcw2025.035.

[20] L. J. Mbigili, N. Nyerere, A. Iddi & S. Mpeshe, "A mathematical analysis of HPV transmission dynamics and cervical cancer progression: The role of screening, prophylactic and therapeutic vaccination strategies", Computer Methods and Programs in Biomedicine Update **8** (2025) 100219. https://doi.org/10.1016/j.cmpbup.2025.100219.

[21] S. Oswald, E. Mureithi, B. Tsanou, M. Chapwanya, C. Kahesa & K. Mashoto, "Mathematical modeling of the impact of hpv vaccine uptake in reducing cervical cancer using a graph-theoretic approach via caputo fractional-order derivatives", Computer Methods and Programs in Biomedicine Update **8** (1) (2025) 100216. https://doi.org/10.1016/j.cmpbup.2025.100216.

[22] I. Al-Shbeil, N. Djenina, A. Jaradat, A. Al-Husban, A. Ouannas & G. Grassi, "A New covid-19 pandemic model including the compartment of vaccinated individuals: Global stability of the disease-free fixed point", Mathematics **11** (2023) 576. https://doi.org/10.3390/math11030576.

[23] O. R. Amanso, N. S. Aguegboh, P. U. Achimugwu, C. A. Okeke, B. E. Chukwuemeka, K. C. Nnamaga & E. O. Oshilim, "Mathematical model of the early incidence and spread of covid-19 in Nigeria combined with control measure", International Journal of Scientific & Engineering Research **11** (2020) 1110.

[24] P. van den Driessche & J. Watmough, "Reproduction numbers and subthreshold endemic equilibria for compartmental models of disease transmission", Mathematical Biosciences **180** (2002) 29. https://doi.org/10.1016/S0025-5564(02)00108-6.

[25] O. Diekmann, J. A. P. Heesterbeek & M. G. Roberts, "Further notes on the basic reproduction number", Mathematical Epidemiology of Infectious Diseases **2** (2010) 159. https://doi.org/10.1007/978-3-540-78911-6_6.

[26] S. Ajao, I. Olopade, T. Akinwumi, S. Adewale & A. Adesanya, "Understanding the transmission dynamics and control of HIV Infection: A mathematical model approach", Journal of the Nigerian Society of Physical Sciences **5** (2023) 1389. https://doi.org/10.46481/jnsps.2023.1389.

[27] O. Diekmann, J. A. P. Heesterbeek & J. A. J. Metz, "On the definition and the computation of the basic reproduction ratio R0 in models for infectious diseases in heterogeneous populations", Journal of Mathematical Biology **28** (1990) 365. https://doi.org/10.1007/BF00178324.

[28] Modeling in Biology contributors, "Dynamical systems analysis of epidemiological models", GitHub pages (2023). https://modelinginbiology.github.io/Dynamical-System-Analysis-of-Epidemiological-Models.

[29] M. Kretzschmar & J. Wallinga, "Mathematical models in infectious disease epidemiology", Modern infectious disease epidemiology (2010) 209. https://doi.org/10.1007/978-0-387-93835-6_12.

[30] A. Sysoev, "Sensitivity analysis of mathematical models", computation **11** (2023) 159. https://doi.org/10.3390/computation11080159.

[31] M. Haddouch, I. Hajjout & E. M. Boudi, "An integrated approach to uncertainty and global sensitivity analysis in penstock structural modeling", Heliyon **11** (2025) 1. https://doi.org/10.1016/j.heliyon.2024.e41049.

[32] S. M. Blower & H. Dowlatabadi, "Sensitivity and uncertainty analysis of complex models of disease transmission: An HIV model, as an example", International Statistical Review **62** (1994) 229. https://doi.org/10.2307/1403510.

[33] O. J. Peter, "Modelling measles transmission dynamics and the impact of control strategies on outbreak management", Journal of Biological Dynamics **19** (2025) 2479448. https://doi.org/10.1080/17513758.2025.2479448.

[34] P. K. Rajan, M. Kuppusamy & O. F. Egbelowo, "A mathematical model for human papillomavirus and its impact on cervical cancer in India", Journal of Applied Mathematics and Computing **69** (2022) 753. https://doi.org/10.1007/s12190-022-01767-2.